



Correction of multi-collector-ICP-MS instrumental biases in high-precision uranium–thorium chronology

Andrew J. Mason*, Gideon M. Henderson

Department of Earth Sciences, University of Oxford, Parks Road, Oxford OX1 3PR, United Kingdom

ARTICLE INFO

Article history:

Received 19 April 2010

Received in revised form 18 June 2010

Accepted 18 June 2010

Available online 8 July 2010

Keywords:

ICP-MS

Thorium isotopes

Chronology

Ion counting

Mass fractionation

ABSTRACT

We present a method for the calibration of in-house thorium isotope standards for use in U–Th chronology, along with an assessment of instrumental biases on the Nu Plasma multi-collector inductively-coupled-plasma mass spectrometer. Uranium and thorium mass fractionation is found to be very strongly coupled, with no evidence of differences in mass bias behaviour. Both Th-isotope and U–Th fractionation are most closely approximated by a linear-law fractionation model. Any deviations from linear law are at the sub-permil level. We also investigate potential biases introduced by intensity-dependant, and ion-beam-path dependant variations in ion-counter response. At count rates $< \sim 350,000$ counts per second, intensity-dependant gain variation can be accounted for entirely by dead-time, while beam-path differences can cause gain variation of up to $\sim 0.8\%$ for different Th isotopes. If this beam-path bias is to be adequately corrected, ion-counter measurements of Th-isotope ratios must be made with reference to bracketing Th-isotope standards measured in the same configuration.

© 2010 Elsevier B.V. All rights reserved.

1. Introduction

Multi-collector inductively coupled plasma mass spectrometry (MC-ICP-MS) has become an important tool in U–Th geochronology [1–3]. Critical to obtaining reliable ages is the ability to accurately and precisely measure sample $^{238}\text{U}/^{234}\text{U}$ and $^{230}\text{Th}/^{238}\text{U}$ ratios, and in some applications the $^{232}\text{Th}/^{230}\text{Th}$ ratio. The $^{238}\text{U}/^{234}\text{U}$ ratio can be measured directly, has much smaller natural variation than the $^{230}\text{Th}/^{238}\text{U}$ ratio and, because well-characterised isotopic reference materials (e.g. [4]) are available for U, instrumental biases can be corrected relatively easily. The $^{230}\text{Th}/^{238}\text{U}$ ratio is measured with reference to a mixed ^{236}U – ^{229}Th , or ^{233}U – ^{229}Th tracer, added to the sample, with the $^{238}\text{U}/^{236}\text{U}$ (or $^{238}\text{U}/^{233}\text{U}$) and $^{230}\text{Th}/^{229}\text{Th}$ ratios typically being measured in separate runs after chemical separation and purification of U and Th. Unlike U, however, suitable well-characterised Th isotope standards are not widely available. Consequently, most labs either use in-house Th standards [10,20], or use U standards to correct for instrumental biases during the measurement of $^{230}\text{Th}/^{229}\text{Th}$ and $^{232}\text{Th}/^{230}\text{Th}$ ratios by ICP-MS [2,5,19].

Mass fractionation (or mass bias) is a prime example of such an instrumental bias. If not adequately corrected, this is a major potential source of inaccuracy in plasma source instrument

measurements and results from the preferential extraction and transmission of heavy ions from the plasma source into the mass spectrometer [6]. For plasma source instruments, mass fractionation is commonly on the order of 0.5–0.8% per atomic mass unit (AMU) in the mass range of U and Th [2]. Correction of mass fractionation requires its magnitude to be assessed by measurement of a solution with a known isotope ratio. While some certified Th standards do exist, such as IRMM-035 and IRMM-036, these have large $^{232}\text{Th}/^{230}\text{Th}$ ratios and lack ^{229}Th , making them unsuitable for this task. The lack of suitable certified standards has led many labs to use the known isotope ratio of certified U standards to correct for Th mass fractionation (e.g. [21]). This approach explicitly relies on U and Th having identical mass fractionation behaviour.

Correcting for isotope fractionation requires knowledge of the behaviour of the isotopes of interest and of the appropriate fractionation 'law' to use. Even for pairs of isotope ratios of a single element, deviation from commonly accepted fractionation laws is observed [17,22,23]. Moreover, studies of element pairs such as Cu–Zn [7] and Tl–Pb [8] suggest elemental differences in mass fractionation behaviour can also occur. Although several causes of mass fractionation in ICP sources has been proposed [6,24], the relative contribution of these effects is uncertain, and mass fractionation remains incompletely understood theoretically, leading many studies to adopt empirical approaches [7,17,22]. It is therefore uncertain as to whether U and Th should exhibit similar mass fractionation behaviour. Previous studies have attempted to evaluate Th versus U mass fractionation on one widely used MC-ICP-MS, the Thermo Fisher Neptune, but results are inconsistent. For exam-

* Corresponding author. Tel.: +44 1865 272000.

E-mail addresses: andrewm@earth.ox.ac.uk, ajm472000@yahoo.com (A.J. Mason).

ple, Ball et al. [9] have suggested differences which could lead to inaccuracies of up to 1% in Th isotope ratios if U is used to correct for Th mass bias, but such large differences are not supported by the work of Hoffman et al. [10].

Another significant analytical bias is the different response of collectors of different type. Most MC-ICP-MS are equipped with Faraday collectors for the measurement of high-intensity signals, and some form of ion-counting system for low-intensity signals. The ion-counter response must be calibrated relative to that of the Faraday collectors prior to analyses, while the response of the ion counter itself is often not directly proportional to signal intensity [11–13]. Hoffman et al. [13] also demonstrated that at least some secondary electron multiplier (SEM) systems have a memory, and that their response to a particular signal is in part determined by the intensity of previously measured signals. Furthermore, Hoffman et al. [10] documented a systematic difference in ion-counter efficiency between U and Th, while both Hoffman et al. [10] and Ball et al. [9] noted similar differences in ion-counter efficiency between U and Th where energy filters were used to improve abundance sensitivity. The low natural abundance of ^{230}Th means that this isotope is usually measured on an ion counting system (as commonly is ^{229}Th – the spike used for isotope dilution) while ^{232}Th is usually measured on a Faraday collector. Consequently, Th isotope ratios are affected by inaccuracies introduced in both the mass bias correction, and any ion-counter bias.

Recent studies of instrumental bias during U and Th analysis for U/Th chronology by MC-ICP-MS have been conducted on the Thermo Neptune. The purpose of the current study is to investigate mass bias and ion-counter biases on the other dominant commercially available MC-ICP-MS – the Nu Plasma MC-ICP-MS – which has a significantly different geometry from the Neptune. The second purpose is to report the calibration of new in-house Th-isotope standards used at the University of Oxford. The study is presented in two parts:

- 1) A combined calibration of in-house thorium standards and assessment of mass-bias behaviour using measurements made entirely on Faraday collectors.
- 2) Assessment of possible sources of inaccuracy from the Nu Plasma ion counting system, based in part on the measurement of the standards calibrated in the first part of the study.

2. Methods

2.1. Instrument design

The design of the Nu Plasma MC-ICP-MS has been described in detail elsewhere (e.g. [14]), and will only be summarised here. The Nu Plasma is a variable-dispersion double-focusing instrument equipped with a fixed array of twelve Faraday collectors and three discrete-dynode ETP ion counters, and operating with an accelerating voltage of ~4 kV. Two quadrupole lenses, which together form a 'zoom' lens, are used to change the dispersion of the instrument, allowing the isotope beams of interest to be aligned with the collector array. Of the three ion counters, one is mounted behind an energy filter designed to reduce peak tailing, and thereby improving abundance sensitivity.

During the present study, analyses were carried out on two separate Nu Plasma instruments at the Dept. Earth Sciences, University of Oxford (with manufacturer product numbers Nu 001 and Nu 010 and termed here 'Plasma 1' and 'Plasma 2' respectively). Both are of Nu Instruments' original low-resolution design. The primary differences between the two instruments are:

- 1) The interface on Plasma-2 is fitted with a larger rotary pump, and hence Plasma-2 has higher ion transmission efficiency than Plasma-1.
- 2) Plasma-1 is equipped with a Cetac Aridus desolvating nebuliser, whereas Plasma-2 is fitted with a Nu Instruments DSN-100 desolvating nebuliser.
- 3) Plasma-1 has an earlier generation of magnet.
- 4) Plasma-1 has less flight-tube baffling.
- 5) The amplifier on the axial Faraday collector on Plasma-1 is fitted with a $10^{10}\ \Omega$ resistor – all other Faraday collectors on both instruments have a $10^{11}\ \Omega$ resistor.

In addition, for one set of measurements (see below) a Thermo Element II single collector ICP-MS was used.

2.2. Thorium isotope standard calibration and mass bias assessment

2.2.1. Standards

Four artificial Th standards have been mixed from separate solutions of ^{232}Th (High Purity Standards Lot # 0724812), ^{230}Th (IRMM 060), ^{229}Th (Eckert & Ziegler Lot # 30216.01 and 'Oak Ridge Th229'). Approximate isotopic composition for these four standards are:

- 1) ThIS-1 $^{232}\text{Th}/^{230}\text{Th} \sim 1$ (with no ^{229}Th)
- 2) ThIS-2 $^{232}\text{Th}/^{230}\text{Th} \sim 1$; $^{230}\text{Th}/^{229}\text{Th} \sim 0.8$
- 3) ThIS-3 $^{232}\text{Th}/^{230}\text{Th} \sim 10^6$; $^{230}\text{Th}/^{229}\text{Th} \sim 0.8$
- 4) MAC-1 $^{232}\text{Th}/^{230}\text{Th} \sim 10$; $^{230}\text{Th}/^{229}\text{Th} \sim 0.06$

One method to make and calibrate such standards is gravimetrically, but high purity ^{232}Th , ^{230}Th and ^{229}Th metal (or oxide) is not readily obtainable, and the stock solutions used here are insufficiently well characterised to allow gravimetric calibration.

ThIS-1 is intended as our primary thorium isotope standard for instrumental tests and for the calibration of additional thorium isotope standards. ThIS-2 and MAC-1 are secondary standards intended for use as bracketing standards in the analysis of real samples. ThIS-3 comprises almost pure ^{232}Th and has a $^{230}\text{Th}/^{229}\text{Th}$ ratio as close as possible to that in ThIS-2. It is intended as a dopant for ThIS-2, such that the $^{232}\text{Th}/^{230}\text{Th}$ ratio of ThIS-2 can be adjusted to match real samples, without significantly changing the $^{230}\text{Th}/^{229}\text{Th}$ ratio. This will allow the mixing of further Th standards with isotope ratios that are a close match to various types of samples.

2.2.2. Instrument setup

Analyses of ThIS-1, ThIS-2, and MAC-1 were carried out on Plasma-2, and ThIS-1 was also analysed on Plasma-1; in some cases these were mixed with CRM U-500 uranium and SRM 982 lead. For results in Sections 3.4–3.6 of the paper, all isotope ratios were measured on Faraday collectors, in blocks of 10×10 -second integrations. Collector baselines were measured prior to each analysis – measurements were made at half masses, and with the electrostatic analyser and transfer optics set to prevent transmission of the ion beam to the collector array. Measurement of baselines after each analysis was also considered, but was unnecessary, due to the relatively short analysis time and the observed stability of the baselines. Collector amplifier gains were calibrated routinely using an internal voltage source, and the deviation of the relative amplifier gains is <20 ppm. Additionally, the relative gains of the Faraday cups themselves were estimated by measuring the $^{207}\text{Pb}/^{206}\text{Pb}$ ratio of SRM981 or SRM982 in different collector pairs. On both instruments, the axial Faraday collector has a relative gain $\neq 1$ (~1.2% high for Plasma-1 and ~0.4% low on Plasma-2), and was avoided. Any deviations in the gain of the other Faradays on Plasma-2 is small (likely to introduce systematic errors of <0.1% if uncorrected), but

has been corrected for. For Plasma-1, the different resistor on the axial collector precluded the reliable measurement of Faraday collector gain at the epsilon-level, and a Faraday gain correction is not applied.

Peak shape, and peak alignment was checked visually every few analyses, or whenever instrument operating parameters were changed. For U–Th and U–Th–Pb mixtures the U, Th, and Pb isotopic ratios were measured alternately. For Pb, this is unavoidable, as it is too light to fit on the collector array with U. U and Th isotope ratios could in principal be measured simultaneously, however, in practice there is sufficient defect in the zoom optics that there is always some compromise in aligning peaks separated by this wide a mass range. For this reason (and since the analysis time is not limited by sample size) U and Th ratios were also measured in alternate steps.

Preliminary tests indicated that in U–Th–Pb mixtures measured on Plasma 1, spuriously scattered ions (predominantly scattered Pb on ^{235}U) produced a small but significant offset in the measured isotope ratios. To correct for this, Th, U, and Pb solutions were analysed separately, so that the contribution of scattered Pb ions to the U and Th measurements could be determined and corrected (and similarly, the effects of scattered Th to the U and Pb measurements etc.). This effect was not observed on Plasma 2 and therefore presumably relates to the less comprehensive flight-tube baffling on the earlier Plasma 1 instrument. Blank contributions from each standard (e.g. trace U and Pb in ThS-1) that would slightly bias the composition of the U–Th–Pb mixtures were corrected in the same way.

Washout times between different solutions was sufficient that memory effects in the measurements are insignificant.

Measurements of ThS-3 were carried out on a Thermo Element II, operating in medium resolution mode. The resolution in this mode is ~ 4000 and is therefore higher than the ~ 400 on the low-resolution Nu Plasma instruments, allowing better characterization of the peak tail of the large ^{232}Th beam. ^{230}Th and ^{229}Th were measured with the collector in counting mode, while ^{232}Th was measured with the collector in analogue mode. The gain between analogue and counting mode is corrected automatically by the instrument software. The mass windows for each isotope was set to 300% of the peak width, so that the contribution of scattered ^{232}Th to the small ^{230}Th and ^{229}Th beams could be assessed on either side of the peak to allow for correction of the peak height.

2.2.3. Procedure for calibration of Th standards

The $^{232}\text{Th}/^{230}\text{Th}$ ratio of ThS-1 has been calibrated against CRM U-500 based on the certified $^{238}\text{U}/^{235}\text{U}$ ratio of $1.0003 \pm 1\%$ for the CRM [4], and an attempted calibration made against NIST SRM982 based on a $^{208}\text{Pb}/^{206}\text{Pb}$ ratio of 1.00016 ± 0.00036 [16]. These calibrations were performed by analysing mixed solutions of ThS-1 and the certified U or Pb standard. Although the Th–Pb fractionation behaviour is not relevant to U–Th chronology, Pb has a similar mass to Th, a well characterised isotopic standard, and provides the most appropriate independent alternative to U for this calibration.

The nature of the $^{238}\text{U}/^{235}\text{U}$ – $^{232}\text{Th}/^{230}\text{Th}$ and $^{208}\text{Pb}/^{206}\text{Pb}$ – $^{232}\text{Th}/^{230}\text{Th}$ fractionation curves is not known *a priori*, and hence to calibrate ThS-1, mass bias must be corrected empirically, without reference to a particular mass fractionation 'law'. The approach taken here is to construct the $^{238}\text{U}/^{235}\text{U}$ – $^{232}\text{Th}/^{230}\text{Th}$ and $^{208}\text{Pb}/^{206}\text{Pb}$ – $^{232}\text{Th}/^{230}\text{Th}$ fractionation curves by making measurements under the largest range of mass fractionation obtainable, and extrapolating them back to zero fractionation for the known standard in the mixture. Under normal running conditions, mass fractionation on the Nu Plasma is on the order of 5–8% per AMU, and the variation in fractionation within a particular analysis session is relatively small (typically $<1.5\%$ /AMU). Manipulation of the desolvator gas flows and torch position can, however, produce a much wider spread of mass bias, between 0.14% and 8.9%/AMU.

Specifically, reducing membrane gas flow, and increasing the spacing between the torch and sampler cone suppresses mass bias (consistent with [6]). Provided flat-topped peak geometry is maintained, the fractionation curves are reproducible.

Producing the widest possible spread of data maximises the likelihood of choosing the appropriate regression method, and minimises uncertainties introduced in extrapolating between the measured data and zero fractionation for the known reference standard (i.e. U-500). However, there is a critical assumption in this method which requires testing: that the measured fractionation curve passes through the true value of the U and Th standard simultaneously (i.e. U fractionation = Th fractionation = 0). To validate the method, two tests were carried out:

- 1) On one of the ThS-1 calibration runs the Th was admixed with SRM982 and the $^{208}\text{Pb}/^{206}\text{Pb}$ – $^{207}\text{Pb}/^{206}\text{Pb}$ fractionation curve was constructed. The $^{208}\text{Pb}/^{206}\text{Pb}$ – $^{207}\text{Pb}/^{206}\text{Pb}$ curve is the simplest possible scenario, since both ratios are between isotopes of the same element (and therefore only subject to mass-dependant effects), and the true value of both ratios is certified. This provides a test of whether, in the absence of any inter-element effects, the method will generate a fractionation curve that passes through the true value of the standard, and hence whether a U–Th fractionation curve is likely to pass through the point where U fractionation = Th fractionation = 0 if there are only mass-dependant effects.
- 2) The second test was to evaluate whether there was any decoupling of U and Th mass fractionation behaviour that could cause deviation from the simple Pb–Pb situation above. ThS-1 calibrations were carried out several times, and on instruments with different configurations to demonstrate reproducibility. If there is any decoupling of U and Th mass fractionation then it is not unreasonable to expect different behaviour on Plasma 1 and Plasma 2 because of their different front-end configurations. Likewise, changing instrument parameters within a particular calibration run (particularly to the extreme running conditions necessary to produce maximum and minimum fractionation values), might be expected to change the fractionation behaviour of Th relative to U at different absolute fractionation values – i.e. the slope of the fractionation curve would change along its length.

Linear regression [15] is used where data sets show no sign of deviation from linearity. From a theoretical standpoint, this is valid, since over the range 0–8.9%/AMU fractionation, all three commonly used fractionation laws give linear (linear law) or insignificantly non-linear (power and exponential laws) theoretical fractionation curves for the U–Th–Pb mixtures used here.

Following calibration of the ThS-1 standard, it was used, in a modified standard bracketing approach, to calibrate the $^{232}\text{Th}/^{230}\text{Th}$ ratios of the two further in house Th standards – ThS-2 and MAC-1. These were also calibrated directly against U-500 in an identical fashion to that described above for ThS-1. At the epsilon level of analytical precision desired here, it cannot be safely assumed that simple standard bracketing with ThS-1 will be adequate to correct for mass fractionation in the unknowns because: (1) irregular temporal drift in mass fractionation will not be fully corrected for; (2) slight systematic differences in the degree of fractionation between the different solutions cannot be ruled out. To help negate these problems, admixed U-500 in both solutions was used to monitor differences in mass fractionation between the unknowns and bracketing ThS-1 standards. The mass fractionation correction was then split into two parts (Appendix A). A first estimate of the mass fractionation for the $^{232}\text{Th}/^{230}\text{Th}$ ratio of the unknown was obtained from the $^{232}\text{Th}/^{230}\text{Th}$ of the bracketing standards; the choice of law is irrelevant since the correction is

Table 1
Summary of calibration results.

	$^{232}\text{Th}/^{230}\text{Th}$	Uncertainty (95% conf.)	$^{230}\text{Th}/^{229}\text{Th}$	Uncertainty (95% conf.)
ThIS-1				
Plasma 1	0.94092	(0.00006)		
Plasma 2 (ThIS-2 calibration run)	0.94096	(0.00005)		
Plasma 2 (MAC1 calibration run)	0.94105	(0.00009)		
Mean	0.94098	0.00064 (0.00014)		
ThIS-2				
Plasma 2	0.95325	0.00065	0.77116	0.00027
MAC1				
Plasma 2	9.9513	0.0069	0.060926	0.000024

Errors are absolute, and include the uncertainty on the certified value of U-500, except those in brackets.

calculated from, and applied to the same ratio. An offset (relative mass bias correction) was then applied to this first fractionation estimate based on the difference in the measured dopant $^{238}\text{U}/^{235}\text{U}$ ratio between the bracketing standard and unknown. This relative mass-bias correction was calculated assuming linear law fractionation, but accounts for <10% of the total mass bias correction on the unknowns, and is consequently insensitive to the choice of fractionation law.

The calibration analyses of ThIS-2 and MAC-1 were made over a wide range of mass fractionation to demonstrate that the modified standard bracketing procedure robustly corrects the unknown to a constant value, irrespective of the magnitude of the mass bias, and also to allow direct comparison to U-500, in the same way that ThIS-1 was calibrated. This dual approach was chosen so that the calibrations of ThIS-2 and MAC-1 are traceable to ThIS-1, as well as to the certified U-500 standard. This allows for potential future refinement of the calibrations for all three standards by measuring ThIS-1 against other primary gravimetric uranium standards.

The $^{230}\text{Th}/^{229}\text{Th}$ ratios of ThIS-2 and MAC-1 were determined in an analogous way to the $^{232}\text{Th}/^{230}\text{Th}$ ratio of ThIS-1, by regression of the fractionation curve, but in this case using the calibrated $^{232}\text{Th}/^{230}\text{Th}$ ratio as a reference point. The $^{230}\text{Th}/^{229}\text{Th}$ ratio of ThIS-3 was determined by standard bracketing (without U doping) using ThIS-2 as the bracketing standard on the Element 2.

2.2.4. Mass bias assessment

The appropriateness of different theoretical mass-fractionation laws has been assessed using data collected during the Th standard calibration runs. Theoretical mass fractionation curves have been calculated for the Th–(U)–(Pb) mixtures, and compared to the observed fractionation curves defined by the measured data. However, it is the slope of the line connecting an analysis to its true value that determines the appropriate fractionation law for that analysis, and this is only guaranteed to be coincident with the measured array if the measured array is both linear and passes through the true isotopic composition. Only measured curves that are considered to meet these requirements are assessed (Th–Pb curves excluded – see Section 3.4).

2.3. Ion counter response and accuracy test

2.3.1. Instrument setup

All ion counter tests were carried out on an ETP electron multiplier on Plasma 2. The high-mass ion counter (ICO) was used, and is not fitted with an energy filter. All three of the ion counters on Plasma 2 are, however, positioned behind a deflector lens such that the ion beam can be automatically deflected if it exceeds a defined intensity, in order to protect the ion counter from damage.

During Th isotope measurement for geochronology, it is usually necessary to measure both the ^{230}Th and ^{229}Th on an ion counter because of the small size of these two beams. On the Nu

Plasma (with its normally supplied collector set-up) this measurement must be made dynamically by switching the ^{230}Th and ^{229}Th into a single ion counter, and accounting for any intensity variation between measurement steps with a normalising isotope (typically ^{232}Th) measured in Faraday collectors in both steps. This creates two potential problems on ICO:

- 1) The response of the ion counter could differ for ^{230}Th and ^{229}Th because of possible mass dependent gain effects (e.g. [9]), or because the beam path of the two isotopes into the ion counter (or through the deflector immediately in front of the ion counter) is subtly different.
- 2) The ^{230}Th and ^{229}Th beam sizes commonly differ in intensity by an order of magnitude, and hence the measured $^{230}\text{Th}/^{229}\text{Th}$ ratio is vulnerable to any intensity-dependant variation in gain.

To quantify the first of these possible problems, a mixture of ^{232}Th , ^{230}Th , ^{229}Th , and ^{236}U was prepared such that the beam intensities of $^{232}\text{Th} \approx ^{230}\text{Th} \approx ^{229}\text{Th} < ^{236}\text{U}$. Faraday/Faraday and Faraday/ICO measurements of the $^{236}\text{U}/^{2xx}\text{Th}$ ratios were then made to determine the gain of ICO when measuring each of the Th isotopes. This mixture was analysed repeatedly, with ion-counter settings and zoom optics re-optimised before each analysis such that the path of the ion beams into ICO were subtly changed. The equal beam size for ^{232}Th , ^{230}Th , and ^{229}Th negates any intensity-dependant response variation.

To test the linearity of the ion counting system, two tests were carried out. Firstly, a series of Faraday/ICO $^{238}\text{U}/^{235}\text{U}$ measurements were made on a natural uranium solution, which was progressively diluted so as to vary the ^{235}U intensity. This was done to qualitatively characterise the ion-counter response curve. The $^{238}\text{U}/^{235}\text{U}$ ratio of natural U was chosen as it is effectively free of memory effects, because only natural U is routinely analysed on Plasma 2 (the U-500 Th standard calibrations were carried out more than a year earlier). This was repeated several times, and runs with obvious temporal drift discarded.

In the second test, ICO/ICO measurements of the $^{230}\text{Th}/^{229}\text{Th}$ ratio and Faraday/ICO measurements of the $^{232}\text{Th}/^{229}\text{Th}$ ratio of MAC-1 (doped to give a $^{232}\text{Th}/^{229}\text{Th} \sim 10$, $^{230}\text{Th}/^{229}\text{Th}$ as per Table 1) were made. ThIS-2 (doped to give a $^{232}\text{Th}/^{230}\text{Th}$ of 249.67 ± 0.42 (95%), $^{230}\text{Th}/^{229}\text{Th}$ as per Table 1) was used as bracketing standard. The $^{230}\text{Th}/^{229}\text{Th}$ and $^{232}\text{Th}/^{229}\text{Th}$ ratios measured for MAC-1 were normalised to the bracketing standards to both correct for mass fractionation, any differences in ion-counter response between ^{230}Th and ^{229}Th aside from intensity-related response differences, and ion-counter-Faraday gain differences. Analyses were made in a two-step routine where the static Faraday/ICO $^{232}\text{Th}/^{230}\text{Th}$ ratio is measured in one step, and the static $^{232}\text{Th}/^{229}\text{Th}$ ratio is measured in the other step, thereby using the Faraday measurement of ^{232}Th to correct for signal instability on the dynamic $^{230}\text{Th}/^{229}\text{Th}$ ratio. The second test was carried out to quantitatively characterise the non-linearity over the intensity range of interest for the

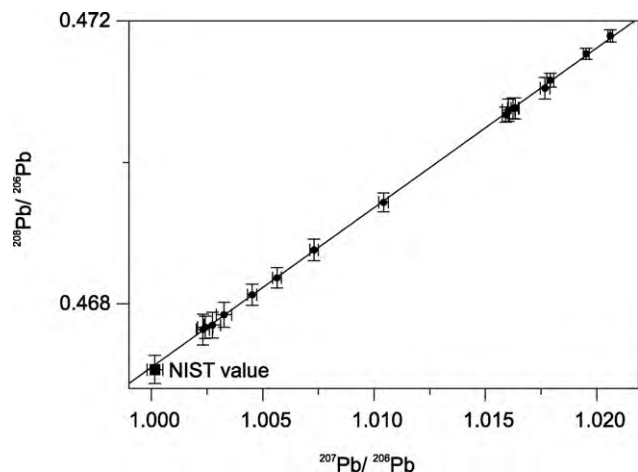


Fig. 1. $^{208}\text{Pb}/^{206}\text{Pb}$ – $^{207}\text{Pb}/^{206}\text{Pb}$ fractionation curve based on SRM982 measurements during the Plasma-1 calibration of ThIS-1. Note that the fractionation curve passes through normally optimised running conditions ($^{208}\text{Pb}/^{206}\text{Pb} \sim 1.016$, $^{207}\text{Pb}/^{206}\text{Pb} \sim 1.017$) and extrapolates to the NIST certified value for SRM982 (shown by the black square). Errors are 2 s.e.

critical $^{230}\text{Th}/^{229}\text{Th}$ ratio, and to determine the accuracy of the non-linearity correction.

3. Results and discussion

3.1. Results – validation of the calibration method

One ThIS-1 – U-500 – SRM982 run was carried out on Plasma-1, and two ThIS-1 – U-500 runs were carried out on Plasma-2, and the data are summarised in Figs. 1–3.

The $^{208}\text{Pb}/^{206}\text{Pb}$ – $^{207}\text{Pb}/^{206}\text{Pb}$ fractionation curve for the SRM982 in the Plasma-1 run forms a linear array, which, when extrapolated passes through the NIST certified value [16] for SRM982 (Fig. 1). Since the curve is both linear, and passes through the true value, the approach of calibrating an unknown standard by

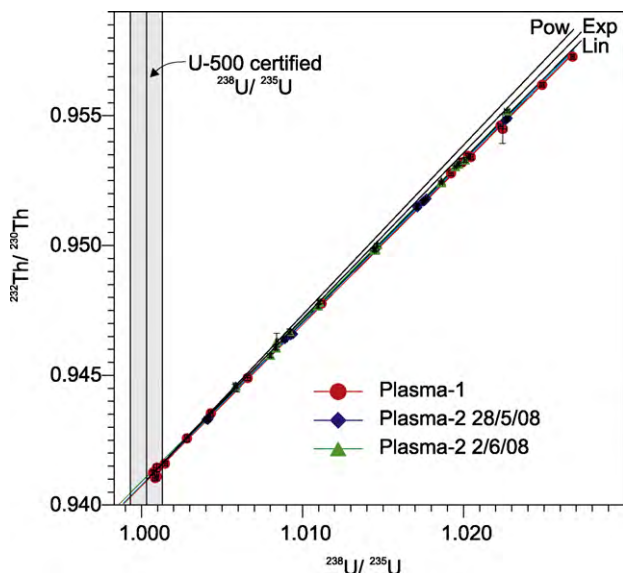


Fig. 2. Calibrations of ThIS-1 against U-500. The vertical line is at 1.0003, the certified $^{238}\text{U}/^{235}\text{U}$ ratio of U-500 [4], and the shaded area is the $\pm 1\%$ uncertainty. The theoretical fractionation curves for the three common fractionation laws, based on a true $^{238}\text{U}/^{235}\text{U}$ of 1.0003, and $^{232}\text{Th}/^{230}\text{Th}$ of 0.94098, are shown for reference. Data with $\sim 1.018 < ^{238}\text{U}/^{235}\text{U} < 1.022$ were obtained under 'normal' operating conditions. Errors are 2 s.e.

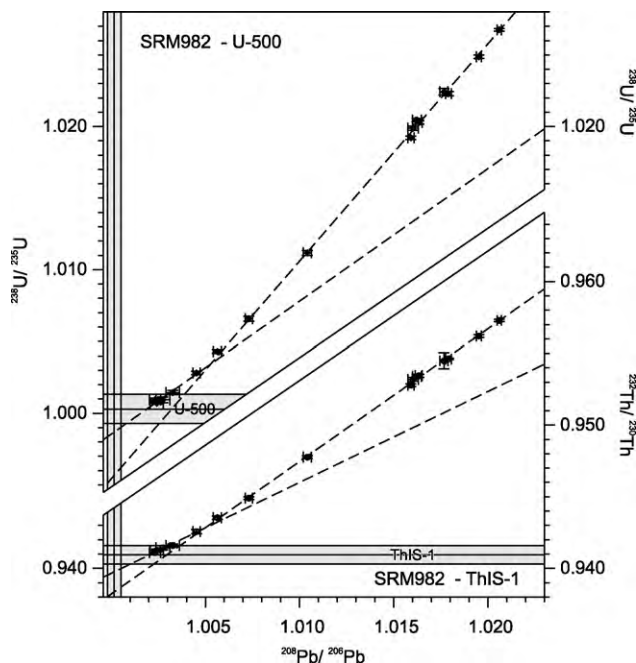


Fig. 3. Pb–Th and Pb–U fractionation curves for an SRM982 – U-500 – ThIS-1 mixture. The vertical shaded region is centred around 1.00016, the certified value of SRM982, and the horizontal shaded regions are the values for the $^{238}\text{U}/^{235}\text{U}$ of U-500, and the best estimate of the $^{232}\text{Th}/^{230}\text{Th}$ ratio of ThIS-1, based on calibration against U-500 (see Fig. 2). Note that for both plots, the curves are non-linear at low fractionation values. The steeper of the regression lines for both plots is fitted through the linear part of the data ($^{208}\text{Pb}/^{206}\text{Pb} > 1.005$), and the flatter curve through the least fractionated data ($^{208}\text{Pb}/^{206}\text{Pb} < 1.005$), and highlights the change in gradient. The slight cluster of data with $\sim 1.016 < ^{208}\text{Pb}/^{206}\text{Pb} < \sim 1.017$ were measured under 'normal' operating conditions. Errors are 2 s.e.

regressing an array of data obtained by deliberately manipulating the mass bias is sound, at least where inter-elemental effects can be ruled out. Furthermore, because the fractionation curve is linear and passes through the true value, the net fractionation path for any individual analysis (i.e. a line connecting an analysis to the true value – the slope of which determines the appropriate fractionation law for correction) is coincident with the measured curve – i.e. the slope of the measured data can be used to assess the fractionation law.

The $^{238}\text{U}/^{235}\text{U}$ – $^{232}\text{Th}/^{230}\text{Th}$ data (Fig. 2) from the three ThIS-1 calibration runs are highly consistent in two respects. Firstly, despite being obtained on instruments with different configurations, all the data define a single coherent curve, and secondly, that curve is linear, and even under the extreme running conditions necessary to produce the high- and low-fractionation parts of the curve, there are no changes in gradient. In other words, U and Th fractionation appear to be strongly coupled – their relative behaviour appears constant irrespective of running conditions or the instrument used for analysis.

Individual ThIS-1 calibration runs have a precision $< 0.1\%$ on the calibrated $^{232}\text{Th}/^{230}\text{Th}$ ratio, and an uncertainty of $< \sim 1\%$ on the fractionation curve slope. We observe no variation outside of analytical uncertainty on either the corrected $^{232}\text{Th}/^{230}\text{Th}$ ratio or the $^{232}\text{Th}/^{230}\text{Th}$ – $^{238}\text{U}/^{235}\text{U}$ fractionation curve slope between the three calibration runs. On this basis, inter-elemental differences in fractionation between U and Th, at least on the nominally pure solutions analysed here, appear unlikely, and it seems a valid assumption that the U–Th curve passes through the point where U fractionation = Th fractionation = 0. This curve therefore simultaneously passes through the true value of the two standards.

In other element pairs, inter-element discrepancies/instability in mass bias has been observed. Thirlwall [8] observed day to day

variations in $^{205}\text{Tl}/^{203}\text{Tl}$ calculated by normalisation to Pb standards of $\sim 0.4\%$, and $\sim 0.3\%$ variations in $^{206}\text{Pb}/^{204}\text{Pb}$ corrected for mass bias using Tl, between different sample introduction systems, both in nominally pure solutions. Maréchal et al. [7] found even larger variations between Cu and Zn with fractionation curve slopes varying by as much as 50% on a day-to-day basis. Both variations are significantly larger than the analytical uncertainty obtained here.

The $^{208}\text{Pb}/^{206}\text{Pb}$ – $^{232}\text{Th}/^{230}\text{Th}$ (and the $^{208}\text{Pb}/^{206}\text{Pb}$ – $^{238}\text{U}/^{235}\text{U}$) data are shown in Fig. 3, and unlike the U–Th data, show non-linearity at low fractionations. The cause for the anomalous behaviour is not known, but the behaviour is not seen in the corresponding $^{208}\text{Pb}/^{206}\text{Pb}$ – $^{207}\text{Pb}/^{206}\text{Pb}$ data and seems to relate to inter-element chemical effects between Pb and Th (and between Pb and U), rather than purely mass-dependent effects.

The bulk of the U–Pb curve (steep line on Fig. 3) has a slope $\sim 3/2$ consistent with the $^{238}\text{U}/^{235}\text{U}$ and $^{208}\text{Pb}/^{206}\text{Pb}$ ratios fractionating coherently together (i.e. the slope at least approximates to ‘normal’ mass bias), but is offset towards greater absolute Pb fractionation relative to U and therefore does not pass through the true value of the standards. The rather flat least fractionated part of the curve provides an indication that at some point in the fractionation path Pb is fractionated in preference to U, and this is borne out by the almost flat trajectories between the least fractionated data and the true value of the standards. The same appears true of Pb and Th. This is consistent with the suggestion of multiple mechanisms for mass fractionation in ICP-MS instruments [24].

The apparent decoupling of Pb and Th fractionation means that the Th–Pb fractionation curve cannot be utilised for calibration purposes (or to assess mass bias law). However, it does demonstrate the value of running the instrument at a wide range of mass biases: interpretation only of the more fractionated linear part of this curve, which includes normal operating conditions, would be misleading.

3.2. Results – thorium standard calibration

Calibration results for ThIS-1 are summarised in Table 1. The $^{238}\text{U}/^{235}\text{U}$ – $^{232}\text{Th}/^{230}\text{Th}$ fractionation curve shows no evidence of non-linearity (Fig. 2), and thus the true value of ThIS-1 has been estimated using linear regression [15] of the data through the certified value for U-500. The three U–Th calibrations yield statistically identical $^{232}\text{Th}/^{230}\text{Th}$ ratios for ThIS-1 with a mean of 0.94098 ± 0.00014 (2SD) (or ± 0.00064 95% including the uncertainty on U-500).

The results for the $^{232}\text{Th}/^{230}\text{Th}$ calibration of ThIS-2 (based on combined U-500 doping and standard bracketing with ThIS-1) are summarised in Table 1. The external reproducibility of the raw ThIS-2 $^{232}\text{Th}/^{230}\text{Th}$ ratios is $\pm 8.24\%$ (2SD), reflecting the wide spread of mass bias. After correction with the modified standard bracketing approach, the corrected $^{232}\text{Th}/^{230}\text{Th}$ ratio is 0.95325 ± 0.00008 (2SD) (or ± 0.00065 95% including the uncertainty on ThIS-1 bracketing standards), and is constant over the range of fractionations obtained (precision improves to $\pm 0.087\%$ (2SD) after correction). A small systematic difference in the mass fractionation between the ThIS-2 analyses and the bracketing ThIS-1 measurements was detected with the U-doping and corrected (mean offset $0.117 \pm 0.058\%$ per AMU, 2SD.). Correction with the Th bracketing standards alone produces a significantly worse external reproducibility of 0.16% (2SD).

Regression of the $^{238}\text{U}/^{235}\text{U}$ – $^{232}\text{Th}/^{230}\text{Th}$ fractionation curve for U-500-doped ThIS-2 (using a value of 1.0003 for U-500) yields a corrected $^{232}\text{Th}/^{230}\text{Th}$ ratio of 0.95326 ± 0.00009 (95%, analytical precision only), within analytical uncertainty of the value obtained by combined standard bracketing and U-doping. The uncertainty on the $^{232}\text{Th}/^{230}\text{Th}$ ratio for ThIS-2 in Table 1 includes the propagated uncertainty on the bracketing standards and Faraday collector gains.

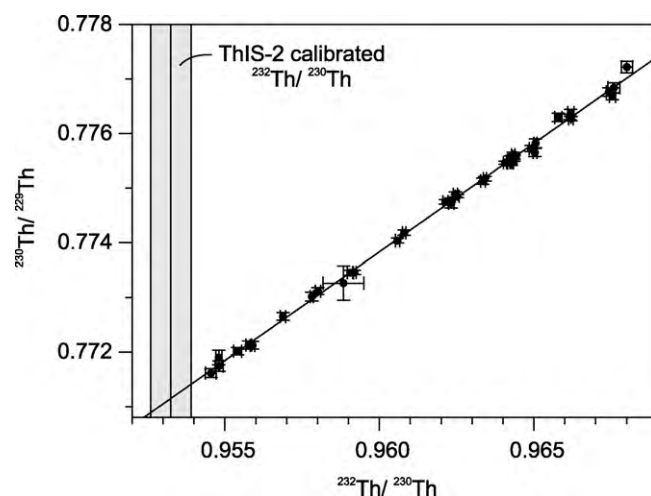


Fig. 4. Calibration of the $^{230}\text{Th}/^{229}\text{Th}$ ratio of ThIS-2 on Plasma-2. 0.95325 ± 0.00065 is the current best estimate of the true $^{232}\text{Th}/^{230}\text{Th}$ ratio of ThIS-2. Errors are 2 s.e.

The results for the $^{230}\text{Th}/^{229}\text{Th}$ calibration of ThIS-2 are summarised in Fig. 4. The data show no evidence of non-linearity, and regression of the $^{232}\text{Th}/^{230}\text{Th}$ – $^{230}\text{Th}/^{229}\text{Th}$ fractionation curve yields a corrected $^{230}\text{Th}/^{229}\text{Th}$ ratio of 0.77116 ± 0.00005 (95%, analytical precision only) (or ± 0.00027 95% including uncertainty from the $^{232}\text{Th}/^{230}\text{Th}$ ratio). For U-500 doped ThIS-2 analyses, regression of the $^{238}\text{U}/^{235}\text{U}$ – $^{230}\text{Th}/^{229}\text{Th}$ fractionation curve yields a value of 0.77112 ± 0.00011 (95%, analytical precision only), identical within analytical error. The $^{230}\text{Th}/^{229}\text{Th}$ value given in Table 1 includes the propagated uncertainty from the $^{232}\text{Th}/^{230}\text{Th}$ ratio of ThIS-2, and Faraday collector gains.

MAC-1 was calibrated in an identical way, also on Plasma 2. The external reproducibility of the raw $^{232}\text{Th}/^{230}\text{Th}$ ratio for MAC-1 is 7% (2SD). Correction with the bracketing standards combined with U-doping gives a value of 9.9513 ± 0.0018 (0.18% 2SD) (or ± 0.0069 95% including the uncertainty on ThIS-1 bracketing standards). No systematic difference in the fractionation between MAC-1 and the bracketing ThIS-1 standards was detected with the U-doping (mean fractionation difference $0.089 \pm 0.200\%$ per AMU 2SD). As in the case of the ThIS-2 calibration, the combined bracketing and doping approach produces better external reproducibility than standard bracketing alone (0.32% versus 0.18% 2SD). Regression of the $^{238}\text{U}/^{235}\text{U}$ – $^{232}\text{Th}/^{230}\text{Th}$ fractionation curve gives an identical value of 9.9501 ± 0.0011 (95%, analytical precision only). The uncertainty on the $^{232}\text{Th}/^{230}\text{Th}$ ratio of MAC-1 presented in Table 1 includes the uncertainty from the bracketing standards and Faraday gains. Regression of the $^{232}\text{Th}/^{230}\text{Th}$ – $^{230}\text{Th}/^{229}\text{Th}$ fractionation curve gives a corrected $^{230}\text{Th}/^{229}\text{Th}$ of 0.060926 ± 0.000014 (95%, analytical precision only) (or ± 0.000024 95% including the uncertainty on the $^{232}\text{Th}/^{230}\text{Th}$ ratio), and regression of the $^{238}\text{U}/^{235}\text{U}$ – $^{230}\text{Th}/^{229}\text{Th}$ fractionation curve gives a corrected $^{230}\text{Th}/^{229}\text{Th}$ of 0.060924 ± 0.000009 (95%, analytical precision only), identical within analytical error. The uncertainty on the $^{230}\text{Th}/^{229}\text{Th}$ ratio of MAC-1 presented in Table 1 includes the uncertainty from the $^{232}\text{Th}/^{230}\text{Th}$ ratio of MAC-1, and Faraday gains.

The $^{230}\text{Th}/^{229}\text{Th}$ ratio of ThIS-3 was calibrated on the Thermo Element 2, using ThIS-2 as the bracketing standard to correct for mass bias; a value of 0.749 ± 0.013 (2SD) was obtained. Abundance sensitivity respectively contributed $\sim 8.5\%$ and $\sim 3.3\%$ to the peak height of ^{230}Th and ^{229}Th . The $^{232}\text{Th}/^{230}\text{Th}$ ratio was also measured as $1.288 \times 10^6 \pm 0.035 \times 10^6$ (2SD) after abundance sensitivity correction, and mass bias correction (linear-law using the $^{230}\text{Th}/^{229}\text{Th}$ ratio). However, the $^{232}\text{Th}/^{230}\text{Th}$ ratio is measured over a large

Table 2

Fractionation curve slopes for various U and Th isotope pairs compared to the theoretical fractionation law slopes according to linear, power, and exponential laws. Errors on the measured slopes are at the 95% confidence limit. The “fit to linear law” is the actual slope divided by the linear law theoretical slope.

	$^{232}\text{Th}/^{230}\text{Th}$ – $^{230}\text{Th}/^{229}\text{Th}$	$^{238}\text{U}/^{235}\text{U}$ – $^{232}\text{Th}/^{230}\text{Th}$	$^{238}\text{U}/^{235}\text{U}$ – $^{230}\text{Th}/^{229}\text{Th}$
ThIS-1		(Fig. 6 point #6)	
Linear	–	0.6271	–
Power	–	0.6549	–
Exponential	–	0.6395	–
Actual	–	0.6241	±0.0037
Fit to linear law	–	0.9952	±0.0059
ThIS-2	(Fig. 6 point #4)	(Fig. 6 point #5)	(Fig. 6 point #3)
Linear	0.4045	0.6353	0.2570
Power	0.4075	0.6634	0.2667
Exponential	0.4048	0.6478	0.2623
Actual	0.3965	0.6299	0.2518
Fit to linear law	0.980	0.9915	0.980
MAC-1	(Fig. 6 point #1)	(Fig. 6 point #7)	(Fig. 6 point #2)
Linear	0.00306	6.632	0.02030
Power	0.00308	6.926	0.02136
Exponential	0.00306	6.763	0.02072
Actual	0.00278	6.740	0.0188
Fit to linear law	0.908	1.016	0.926

dynamic range, and it was not possible to standard bracket to account for any non-linearity of the SEM collector, hence, this value is as an approximation only.

3.3. Results – assessment of mass fractionation law

York [15] regression slopes for $^{238}\text{U}/^{235}\text{U}$ – $^{232}\text{Th}/^{230}\text{Th}$, $^{238}\text{U}/^{235}\text{U}$ – $^{230}\text{Th}/^{229}\text{Th}$, and $^{232}\text{Th}/^{230}\text{Th}$ – $^{230}\text{Th}/^{229}\text{Th}$ fractionation curves are summarised in Table 2, along with the theoretical slopes of the fractionation curves according to the commonly assumed mass fractionation laws (the method for calculating the theoretical slopes is given in Appendix A). Measurements fall on straight lines and are considered in all cases to pass through the true isotopic composition, therefore fulfilling the requirements to meaningfully assess their slopes and hence the most appropriate fractionation law. Overall, the linear law is the best approximation to the data and provides a good fit to most datasets. Deviations from linear law are apparent, however, particularly for combinations of the MAC-1 standard and U-500 where the $^{238}\text{U}/^{235}\text{U}$ – $^{232}\text{Th}/^{230}\text{Th}$ relationship is ~1.6% steeper than the theoretical linear-law slope, while the $^{238}\text{U}/^{235}\text{U}$ – $^{230}\text{Th}/^{229}\text{Th}$ relationship is ~7.3% shallower. The deviation from linear law (and similarly for exponential law) appears to be non-random (Fig. 5), and varies systematically with the slope of the measured fractionation curve. Note that the $^{208}\text{Pb}/^{206}\text{Pb}$ – $^{207}\text{Pb}/^{206}\text{Pb}$ fractionation curve also falls on the same trend.

Figure 6 documents the slight breakdown of linear law fractionation in MAC-1. The deviation between uranium corrected $^{230}\text{Th}/^{229}\text{Th}$ ratios, and the calibrated $^{230}\text{Th}/^{229}\text{Th}$ increases with increasing fractionation. However, it should be noted, that while using U to correct for Th mass bias is detectably inaccurate for MAC-1, the inaccuracy in the corrected ratio is at worst <0.7%, and under more typical fractionation values of 5% per AMU is <0.5%. At the permit level of precision typical of ^{230}Th measurements the use of U to correct for mass bias assuming linear law is a reasonable approximation on the Nu Plasma (consistent with the conclusions of Hoffman et al. [10] for the Thermo Neptune).

At the epsilon level precision, obtainable by some recent studies in which modified Faraday collectors have been used in place of ion counters [18], such variations in mass fractionation law are potentially significant. Variations in fractionation law between different isotope ratio pairs have been documented previously for Nd, and Cd and Sn, along with methods for dealing with such anomalies [17,23]. Given that the deviation from linear law observed here

shows some evidence of being systematic, a somewhat analogous method for correction is suggested, whereby a basic fractionation law is modified with a secondary correction. Examination of Fig. 5 reveals that the deviation from linear law only changes significantly with decadal variation in fractionation curve slope, and therefore even a crude estimate of the slope of the fractionation curve could be used to refine the fractionation law used. This is significant

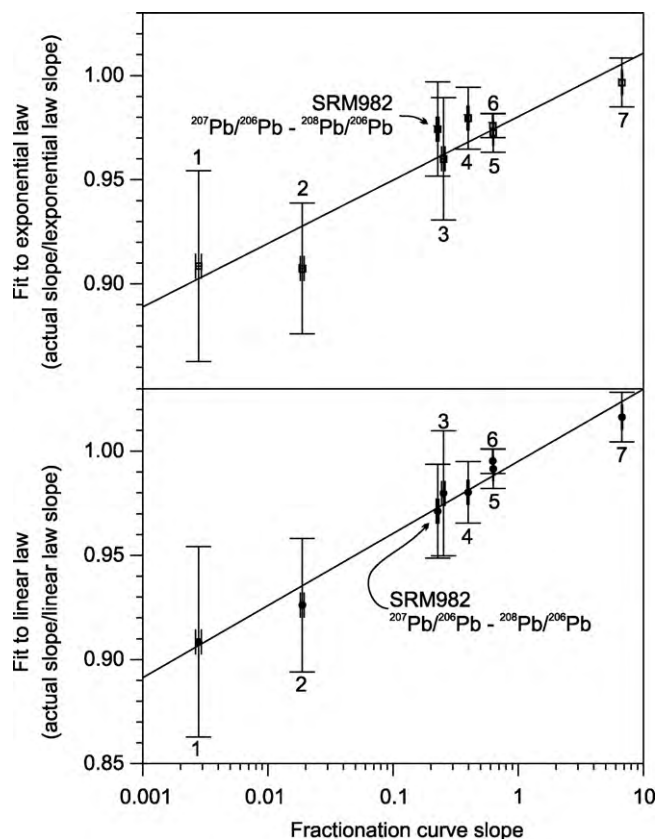


Fig. 5. Deviation in slope of measured $^{238}\text{U}/^{235}\text{U}$ – $^{232}\text{Th}/^{230}\text{Th}$, $^{238}\text{U}/^{235}\text{U}$ – $^{230}\text{Th}/^{229}\text{Th}$, and $^{232}\text{Th}/^{230}\text{Th}$ – $^{230}\text{Th}/^{229}\text{Th}$ fractionation curves from the theoretical linear law and exponential law slopes. Note that the deviation is non-random and correlates with the slope of the fractionation curve. Errors are 2 s.e. The reference numbers for the data points correspond to those in Table 2. The slope for the $^{208}\text{Pb}/^{206}\text{Pb}$ – $^{207}\text{Pb}/^{206}\text{Pb}$ fractionation curve from SRM982 obtained during ThIS-1 calibration is also shown, and falls on the same trend.

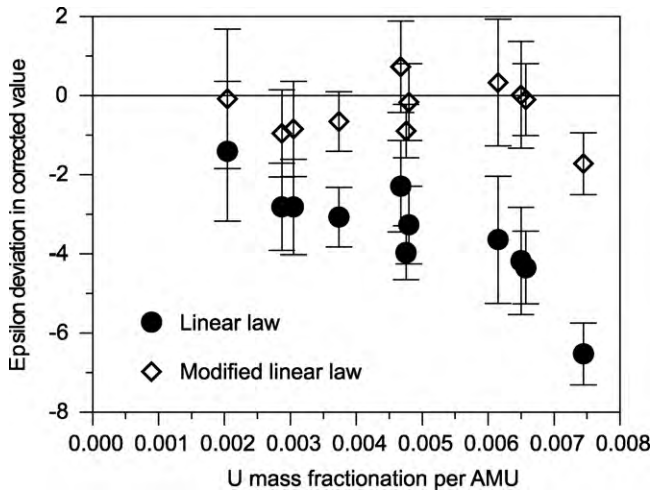


Fig. 6. Deviation of $^{230}\text{Th}/^{229}\text{Th}$ ratios, corrected using linear law mass bias calculated from $^{238}\text{U}/^{235}\text{U}$, from the calibrated value for MAC-1. The modified linear law correction used here applies 0.935 of the linear law U fractionation to the Th. The value of 0.935 is read from Fig. 5 based on a $^{238}\text{U}/^{235}\text{U}$ – $^{230}\text{Th}/^{229}\text{Th}$ fractionation curve slope estimate of ~ 0.02 , obtained from the raw data. Note that the deviation is substantially reduced. Errors are 2 s.e.

because for unknowns it means that an estimate of the theoretical linear law slope can be calculated from the raw measured data, and used to determine an offset from linear law to refine the correction. An example of such a correction is illustrated in Fig. 6.

3.4. Results – ion counter biases

Ion counter gain is seen to differ between Th isotopes by $\sim 0.8\%$ (Fig. 7). This variation is not seen to be systematic with respect to mass, but does change on re-optimizing the zoom optics/ion-counter settings, suggesting the change in beam path is responsible for this effect. This finding is significant because beam-path effects could potentially bias all dynamic ion-counter measurements, not

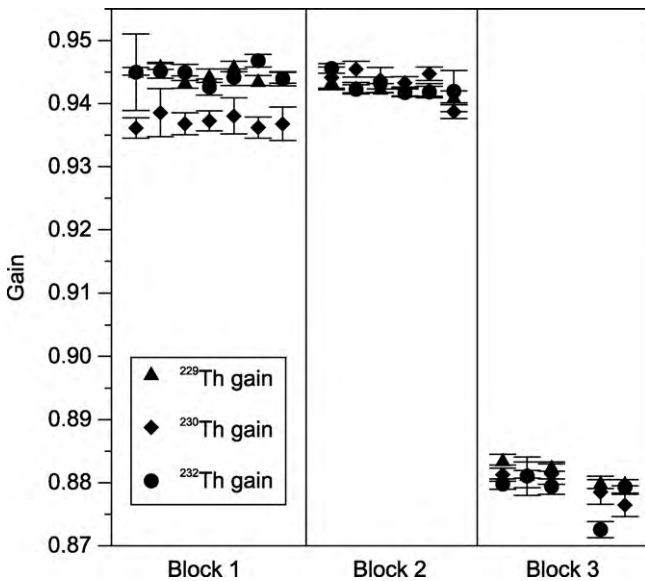


Fig. 7. Gain for different Th isotopes determined by measuring $^{2xx}\text{Th}/^{236}\text{U}$ alternately on IC0/Faraday and Faraday/Faraday for each Th isotope. Data were collected in three blocks; the ion counter was re-tuned before each block. Note that in the first block of data the gain for ^{230}Th is $\sim 0.8\%$ lower than that for ^{232}Th and ^{229}Th . This difference is not systematic with respect to mass, and is absent in the subsequent blocks after re-optimisation of the zoom optics and ion counter settings. Errors are 2 s.e.

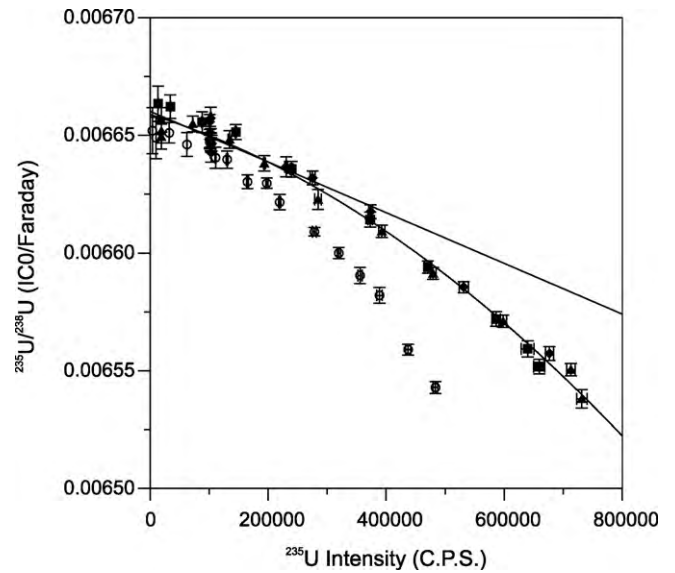


Fig. 8. Faraday/IC0 measurements of $^{235}\text{U}/^{238}\text{U}$ versus ^{235}U signal intensity on IC0. The data are raw, and uncorrected for gain, mass fractionation, or dead-time of the ion-counter system; measurements were made by progressively diluting a natural U solution to change the signal intensity, and constitute four replicate runs. The first run (open symbols) is not coincident with the subsequent runs (probably due to temporal drift in the gain) and is not considered further. The response curve $< \sim 350,000$ cps is not significantly non-linear, however, the slope clearly increases at higher count rates. Errors are 2 s.e.

only those of U–Th, and the only obvious way of determining that such effects are not present (or correcting for them if they are), is by standard bracketing. For Th measurements for chronology, this means that the critical $^{230}\text{Th}/^{229}\text{Th}$ ratio must be bracketed with $^{230}\text{Th}/^{229}\text{Th}$ measurements of known standards, and it also effectively precludes the use of U for determining ion counter gain

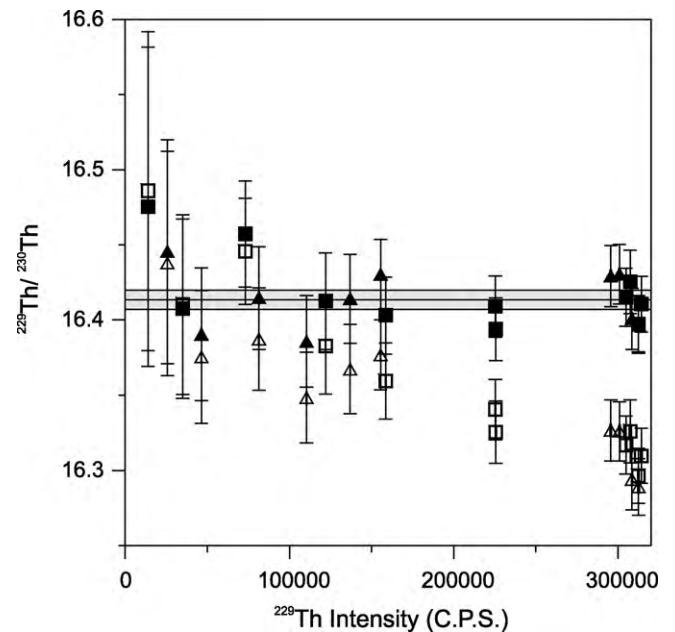


Fig. 9. Measurements of MAC-1 $^{229}\text{Th}/^{230}\text{Th}$ on IC0 versus ^{229}Th intensity. Open symbols are corrected for all biases except dead-time, using THS-2 bracketing standards (two runs on consecutive days). Filled symbols are the same data with a 22.7 ± 2.2 ns dead-time correction applied. Note the slope on the non-dead-time corrected data, and the inaccuracy of the values obtained above $\sim 100,000$ cps. The horizontal shaded region corresponds to the calibrated value of MAC-1. Errors are 2 s.e.

during Faraday/ion-counter $^{232}\text{Th}/^{230}\text{Th}$ measurement where high accuracy is required.

Assessment of ICO response reveals a gain decreases of $\sim 2\%$ across count rates from close to zero to 800,000 cps (Fig. 8). At count rates $< 350,000$ cps, this decrease can be fitted by a straight line. At higher count rates the slope of the response curve clearly changes (Fig. 8), but this is above the intensity range at which ion-counter measurements are routinely made (350,000 cps is equivalent to ~ 5.6 mV allowing straightforward Faraday measurement). Below $\sim 350,000$ cps, the change in gain with intensity can be well explained by a dead-time in the ion-counter system of ≈ 22 ns.

This dead-time was more quantitatively constrained using fully standard bracketed measurements of MAC-1, up to ^{229}Th intensities of 350,000 cps (i.e. corresponding to the linear part of Fig. 8). The Faraday/ICO $^{232}\text{Th}/^{229}\text{Th}$ and ICO/ICO $^{230}\text{Th}/^{229}\text{Th}$ data both show an increase in ratio with signal intensity. This linear increase of ratio with signal intensity is removed by applying a 22.7 ± 2.2 ns dead-time (Fig. 9).

4. Conclusions

This study demonstrates that Th standards can be robustly calibrated against known U standards without the need to assume a fractionation law. Such calibrated Th standards are critical to understanding and fully correcting instrumental biases in Th isotope measurements.

Linear law mass bias provides a reasonable approximation for U–Th and Th mass fractionation and, under typical running conditions, its use is likely to lead to inaccuracies of $< 0.5\%$. In principle, therefore, U can reasonably be used to correct mass bias during the analysis of unknown Th samples at the permil level of precision typical of most ion counter analyses. At higher precision, deviation from linear law becomes significant, but is potentially correctable as the deviation apparently varies systematically with respect to fractionation curve slope.

In practice, solely using U to correct for mass fractionation is not convenient for dynamic ion counter measurements of $^{230}\text{Th}/^{229}\text{Th}$ on the Nu Plasma. This ratio is potentially biased by beam-path effects leading to gain differences on the ^{230}Th and ^{229}Th measurements at permil level or larger. Variation in SEM gain between different isotopes has been observed previously, and especially between U and Th isotopes where an energy filter is used [9,10]. Although not investigated here, this is a similar problem to that of differing beam-path effects presented here – i.e. ion counter response can vary between different isotope beams. Such biases on unknown samples can only be corrected using Th standards measured in the same configuration, and it is therefore more practical to standard bracket samples with Th standards, applying a combined correction for mass bias and ion counter response.

Under the typical operating range of 0 to $\sim 350,000$ cps used for ^{230}Th and ^{229}Th measurements, all non-linearity on the ETP electron multiplier tested here can be explained by dead-time.

Acknowledgements

Drs. Nick Belshaw and Alex Thomas are thanked for useful discussion of the data and constructive comments on the manuscript. An anonymous reviewer is also thanked for helpful comments.

Appendix A.

Correction procedure used in the combined ThIS-1 standard bracketing – U-500 doped calibration of the $^{232}\text{Th}/^{230}\text{Th}$ ratio of ThIS-2 and MAC1:

Relative mass bias per AMU between unknown standard and bracketing standard is calculated:

$$\text{relative_mass_bias} = ((238\text{U}_{235}\text{un}/\text{mean}_{238\text{U}_{235}\text{bra}}) - 1)/3$$

where $238\text{U}_{235}\text{un}$ is the measured $^{238}\text{U}/^{235}\text{U}$ ratio of the U-500 doped unknown standard (i.e. ThIS-2 or MAC-1), and $\text{mean}_{238\text{U}_{235}\text{bra}}$ is the mean measured $^{238}\text{U}/^{235}\text{U}$ ratio of the two bracketing standards (U-500 doped ThIS-1).

The absolute mass bias per AMU of the $^{232}\text{Th}/^{230}\text{Th}$ of bracketing standards (U-500 doped ThIS-1) is calculated:

$$\text{absolute_mass_bias} = ((\text{Measured}_{232\text{Th}_{230}}/\text{True}_{232\text{Th}_{230}}) - 1)/2$$

where the true $^{232}\text{Th}/^{230}\text{Th}$ ratio of ThIS-1 is taken as 0.94098 ± 0.00064

The mass bias per AMU of the $^{232}\text{Th}/^{230}\text{Th}$ of the unknown standard is estimated:

$$\text{corrected_mass_bias} = \text{mean_abs_mb_bra} + \text{relative_mass_bias}$$

where mean_abs_mb_bra is the mean of the absolute mass bias of the two bracketing standards.

The unknown standard is then corrected:

$$\text{corr_ratio} = \text{meas_ratio}/(1 + 2 \times \text{corrected_mass_bias})$$

where corr_ratio is the corrected $^{232}\text{Th}/^{230}\text{Th}$ ratio and meas_ratio is the measured $^{232}\text{Th}/^{230}\text{Th}$ ratio.

Note that although linear law is used to calculate the absolute mass bias, the choice of fractionation law is unimportant because the correction is both derived from, and applied to the same ratio.

Calculation of theoretical linear law slope for U–Th fractionation lines:

$$\text{slope} = (\text{true_Th_ratio}/\text{true_U_ratio}) \times (\Delta\text{mass_Th}/\Delta\text{mass_U})$$

Where true_Th_ratio is the true thorium isotope ratio (i.e. $^{232}\text{Th}/^{230}\text{Th}$ or $^{230}\text{Th}/^{229}\text{Th}$ ratio), true_U_ratio is the true uranium isotope ratio (i.e. $^{238}\text{U}/^{235}\text{U}$ ratio of U-500), $\Delta\text{mass_Th}$ is the nominal mass difference between the thorium denominator and numerator isotope, and $\Delta\text{mass_U}$ is the nominal mass difference between the uranium denominator and numerator isotope.

Calculation of theoretical slopes for exponential and power laws:

The slopes have been calculated using the appropriate forms of the generalised power given in Maréchal et al. [7]. Synthetic ‘measured’ data based on the certified value for U-500 and the calibrated values of ThIS-1, ThIS-2, and MAC-1 were then generated over the range of 0 to ~ 9 per AMU, and a linear fit used to approximate the slope. Note over the range of interest, both the exponential and power laws deviate insignificantly from linearity.

References

- [1] C.H. Stirling, T.M. Esat, K. Lambeck, M.T. McCulloch, S.G. Blake, D.-C. Lee, A.N. Halliday, Orbital forcing of the marine isotope stage 9 interglacial, *Science* 291 (2001) 290–293.
- [2] L.F. Robinson, G.M. Henderson, N.C. Slowey, U–Th dating of marine isotope stage 7 in Bahamas slope sediment, *Earth and Planetary Science Letters* 196 (2002) 175–187.
- [3] G.M. Henderson, L.F. Robinson, K. Cox, A.L. Thomas, Recognition of non-Milankovitch sea-level highstands at 185 and 343 thousand years ago from U–Th dating of Bahamas sediment, *Quaternary Science Reviews* 25 (2006) 3346–3358.
- [4] E.L. Garner, L.A. Machlan, W.R. Shields, Standard reference materials: uranium isotopic standard reference materials, National Bureau of Standards Special Publication 260–27 (1971) 1–150.
- [5] J. Hellstrom, Rapid and accurate U/Th dating using parallel ion-counting multi-collector ICP-MS, *Journal of Analytical Atomic Spectrometry* 18 (2003) 1346–1351.
- [6] H. Andrén, I. Rodushkin, A. Stenberg, D. Malinovsky, D.C. Baxter, Sources of mass bias and isotope ratio variation in multi-collector ICP-MS: optimization of instrumental parameters based on experimental observations, *Journal of Analytical Atomic Spectrometry* 19 (2004) 1217–1224.

- [7] C.N. Maréchal, P. Télouk, F. Albarède, Precise analysis of copper and zinc isotopic compositions by plasma-source mass spectrometry, *Chemical Geology* 156 (1999) 251–273.
- [8] M.T. Thirlwall, Multicollector ICP-MS analysis of Pb isotopes using a ^{207}Pb – ^{204}Pb double spike demonstrates up to 400 ppm/amu systematic errors in Tl-normalisation, *Chemical Geology* 184 (2002) 255–279.
- [9] L. Ball, K.W.W. Sims, J. Schwieters, Measurement of $^{234}\text{U}/^{238}\text{U}$ and $^{230}\text{Th}/^{232}\text{Th}$ in volcanic rocks using the Neptune MC-ICP-MS, *Journal of Analytical Atomic Spectrometry* 23 (2008) 173–180.
- [10] D.L. Hoffmann, J. Prytulak, D.A. Richards, T. Elliott, C.D. Coath, P.L. Smart, D. Scholz, Procedures for accurate U and Th isotope measurements by high precision MC-ICPMS, *International Journal of Mass Spectrometry* 264 (2007) 97–109.
- [11] S. Richter, S.A. Goldberg, P.B. Mason, A.J. Traina, J.B. Schwieters, Linearity tests for secondary electron multipliers used in isotope ratio mass spectrometry, *International Journal of Mass Spectrometry* 206 (2001) 107–127.
- [12] K.H. Rubin, Analysis of $^{232}\text{Th}/^{230}\text{Th}$ in volcanic rocks: a comparison of thermal ionisation mass spectrometry and other methodologies, *Chemical Geology* 175 (2001) 723–750.
- [13] D.L. Hoffmann, D.A. Richards, T.R. Elliott, P.L. Smart, C.D. Coath, C.J. Hawkesworth, Characterisation of secondary electron multiplier nonlinearity using MC-ICPMS, *International Journal of Mass Spectrometry* 244 (2005) 97–108.
- [14] N.S. Belshaw, P.A. Freedman, R.K. O’Nions, M. Frank, Y. Guo, A new variable dispersion double-focusing plasma mass spectrometer with performance illustrated for Pb isotopes, *International Journal of Mass Spectrometry* 181 (1998) 51–58.
- [15] D. York, Least squares fitting of a straight line with correlated errors, *Planetary Science Letters* 5 (1969) 320–324.
- [16] E.J. Catanzaro, T.J. Murphy, W.R. Shields, E.L. Garner, Absolute isotopic abundance ratios of common, equal-atom, and radiogenic lead isotopic standards, *Journal Resources of the National Bureau of Standards* 72A (1968) 261–267.
- [17] D. Vance, M. Thirlwall, An assessment of mass discrimination in MC-ICPMS using Nd isotopes, *Chemical Geology* 185 (2002) 227–240.
- [18] E.-K. Potter, C.H. Stirling, M.B. Andresen, A.N. Halliday, High precision Faraday collector MC-ICPMS thorium isotope ratio determination, *International Journal of Mass Spectrometry* 247 (2005) 10–17.
- [19] A.J. Pietruska, R.W. Carlson, E.H. Hauri, Precise and accurate measurement of ^{226}Ra – ^{230}Th – ^{238}U disequilibria in volcanic rocks using plasma ionization multicollector mass spectrometry, *Chemical Geology* 188 (2002) 171–191.
- [20] S. Turner, P. van Calsteren, N. Vigier, L. Thomas, Determination of thorium and uranium isotope ratios in low-concentration geological materials using a fixed multi-collector-ICP-MS, *Journal of Analytical Atomic Spectrometry* 16 (2001) 612–615.
- [21] X. Luo, M. Rehkämper, D.-C. Lee, A.N. Halliday, High precision $^{230}\text{Th}/^{232}\text{Th}$ and $^{234}\text{U}/^{238}\text{U}$ measurements using energy-filtered ICP magnetic sector multiple collector mass spectrometry, *International Journal of Mass Spectrometry and Ion Processes* 171 (1997) 105–117.
- [22] C.P. Ingle, B.L. Sharp, M.S.A. Horstwood, R.R. Parrish, D.J. Lewis, Instrument response functions, mass bias and matrix effects in isotope ratio measurements and semi-quantitative analysis by single and multi-collector ICP-MS, *Journal of Analytical Atomic Spectrometry* 18 (2003) 219–229.
- [23] F. Wombacher, M. Rehkämper, Investigation of the mass discrimination of multiple collector ICP-MS using neodymium isotopes and the generalise power law, *Journal of Analytical Atomic Spectrometry* 18 (2003) 1371–1375.
- [24] K.G. Heumann, S.M. Gallus, G. Rädlinger, J. Vogl, Precision and accuracy in isotope ratio measurement by plasma source mass spectrometry, *Journal of Analytical Atomic Spectrometry* 13 (1998) 1001–1008.